PS reflection-based full-waveform inversion using single-mode propagator

Yongbo Zhai, James Xu, James Rickett, Peng Wang, Xin Cheng, Denes Vigh, Suyang Chen and Cara Smith, SLB*

Summary

Full-waveform inversion (FWI) has emerged as an effective technique for revealing subsurface structures through improved earth model building. However, the predominant focus has been on constructing pressure (P)-wave velocity models, while modeling of the shear (S) wave velocity remains challenging and often overlooked. Although full elastic modeling allows us to simulate all major seismic phases, including S-waves, its computational cost is substantial compared to acoustic modeling. Additionally, isolating the S-wave velocity update from full elastic modeling remains a challenging task. In this study, we introduce a robust FWI approach that leverages PS converted waves to update shear velocity using single-mode propagators. Despite a slight reduction in accuracy, we successfully simulate PS converted waves by solving an approximated S-wave equation. By employing different imaging conditions, we update both the high-wavenumber and low-wavenumber components of the S-wave velocity. Synthetic and field data examples demonstrate that our proposed method effectively addresses the gap in S-wave velocity model building (VMB), advancing our understanding of subsurface properties.

Introduction

Full-waveform inversion (FWI) is a powerful imaging technique that uses complete waveform data to explore subsurface structures, preserving both phase and amplitude information. While most FWI applications have focused on updating P-wave velocities, recent research has delved into elastic modeling to account for S-wave effects (Pratt et al., 1998, Cheng et al., 2016, Dutta et al., 2023, Glaccum et al., 2023). However, conventional FWI faces challenges when dealing with recorded data lacking long-offset refracted energy, making it difficult to determine the correct update direction. To tackle this, Sun et al. (2016) proposed a reflection-based FWI scheme that efficiently updates the low-wavenumber background of P-velocity models without relying on long-offset refractions.

Despite the successful application of FWI in constructing P-wave velocity models, the development of shear velocity models has received less attention. The challenges stem from acquiring and processing shear-wave data. Conventional shear velocity model building (VMB) relies on joint PP-PS tomography and event registration. Similar to P-wave tomography, PP-PS joint tomography aims to flatten both PP and PS common-image gathers, improving velocity models by mitigating residual moveout errors. However, it shares limitations with conventional P-wave tomography, including poor illumination and the inability to resolve multi-arrivals. Additionally, in complex geological areas, the ray-tracing method yields unreliable and unstable common image point offset picks. Event registration is vital for aligning PP and PS events at the same depth in the joint tomography. The 'displacement field' represents the depth difference between these events and provides flexible constraints to minimize discrepancies in the PP and PS images. Nevertheless, this approach has limitations, especially when dealing with poor-quality PS events.

The pursuit of a comprehensive solution for shear VMB has led researchers to explore full-elastic modeling and inversion. Vigh et al. (2023) demonstrated the efficacy of multiparameter elastic FWI using sparse ocean-bottom node data to accurately update P-velocity models near salt bodies. However, this approach comes with a relatively high computational cost due to its inherent complexity. Furthermore, in the context of elastic modeling, which encompasses both P and S events, the challenge lies in separating their individual contributions during conventional elastic FWI. In this paper, we introduce a novel approach that uses single-mode propagators to simulate both P and S waves. We apply the Born approximation to model P-to-S converted waves, which we then compare with field data for shear velocity inversion. Leveraging existing P-wave solvers allows straightforward S-wave simulation with minor code adjustments, maintaining computational efficiency without compromising quality. The method yields pure P-to-S conversions and promises robust and accurate shear velocity updates. Synthetic tests demonstrate its effectiveness even with limited data coverage. Additionally, we apply this approach to real data from the North Sea, revealing previously undisclosed details in updated shear velocity models.

Theory

PS Born modeling

The PS Born modeling procedure adheres to the standard Born approximation, as derived by Dai et al. (2012). Specifically, we begin by considering the acoustic TTI wave equation formulation proposed by Fletcher et al. (2009). By perturbing the background wavefields, denoted as p_0 and q_0, along with the background velocity V_{pz}, we linearize the equation to obtain the TTI Born equations:

$$\frac{\partial^2 \delta p}{\partial t^2} - V_{px}^2 H_2 \delta p - V_{pz}^2 H_1 \delta q - V_{sz}^2 H_1(\delta p - \delta q) = m\frac{\partial^2 p_0}{\partial t^2}$$
$$\frac{\partial^2 \delta q}{\partial t^2} - V_{pn}^2 H_2 \delta p - V_{pz}^2 H_1 \delta q + V_{sz}^2 H_2(\delta p - \delta q) = m\frac{\partial^2 q_0}{\partial t^2} \quad (1)$$

where δp and δq are scattered wavefields, respectively. m is the reflectivity provided by the user. H_1 and H_2 are the operators following Fletcher, et al (2009). In a typical PS simulation, we solve for the background fields p_0 and q_0 using acoustic P-wave anisotropy parameters. The scattered wavefields are then computed using the aforementioned Born equations, incorporating anisotropic parameter substitutions as described in subsequent sections. In the reciprocal scenario, the background wavefields correspond to S-waves, while the scattered wavefields represent P-waves.

S-wave anisotropy

Transverse isotropy (TI) manifests differently in P and S-wave propagation. To address this, we apply the Thomsen trick—a technique previously employed in PSTTI (P-SV Transversely Isotropic) RTM. The Thomsen trick allows us to convert S-wave anisotropy parameters to their P-wave counterparts, enabling accurate S-wave propagation.

Under the assumption of weak TI anisotropy, we express the dependence of P and S velocities in terms of the angle from the symmetry axis (Thomsen, 1986):

$$v_p^2 \approx v_{pz}^2[1 + 2\varepsilon \sin^2\theta - 2(\varepsilon - \delta)\sin^2\theta\cos^2\theta]$$
$$v_{sv}^2 \approx v_{sz}^2[1 + 2\sigma \sin^2\theta\cos^2\theta] \quad (2)$$

where $\sigma = \frac{v_{pz}^2}{v_{sz}^2}(\varepsilon - \delta)$.

Making the substitutions, $\hat{v}_{pz} \leftarrow v_{sz}$, $\hat{\varepsilon} \leftarrow 0$, $\hat{\delta} \leftarrow \sigma$, we modify the TTI pseudo-acoustic wave propagator to model S-wave kinematics. Although the accuracy of S-wave propagation is generally acceptable, it may degrade under certain conditions, e.g., with strong anisotropy or S-wave triplication missing.

Reciprocity

In the physical world, typical scenarios involve a pressure source within the water column, and shear waveforms are measured using geophones or similar devices, resulting in a PS (pressure-shear) experiment. However, during inversion or imaging processes, there are computational advantages to adopting the reciprocal approach. In this context, we model shear propagation using an S-source and measure pressure responses (an SP experiment). To accommodate flexibility, our implementations support both physical and reciprocal modeling. Specifically, we can simulate shear waves either on the source leg (SP) or on the receiver leg (PS), allowing for versatile exploration of subsurface properties.

Choice of objective functions

The simulated PS reflection data can be directly compared to the observed input data using a least-squares or alternative objective functions. However, due to the limitations of single-mode propagators in accurately modeling amplitudes (including zero-offset phase reversals), it becomes necessary to normalize amplitudes or employ an objective function that is insensitive to amplitude variations. The enhanced template matching (ETM) objective function, as proposed by Cheng et al. (2023), serves this purpose effectively.

The adjoint source can then be computed based on the chosen objective function, and standard optimization algorithms such as steepest descent, conjugate gradients, or LBFGS can be employed to minimize the objective function and converge toward an S-velocity model that aligns with the observed data. The P-velocity model remains unaltered during the inversion. However, as the S-velocity model evolves, adjustments to the PS reflectivity model may become necessary—either through repositioning or regeneration—to ensure consistency with the data used in the inversion, especially across different frequency bands.

Preprocessing requirements are similar to those of PSTTI RTM. Specifically, the input data should have multiples removed (due to the Born approximation dependency), and zero-offset polarity reversal should be addressed. Additionally, optimizing the workflow involves mitigating the impact of very slow shear velocities near the seafloor, potentially excluding these from the FWI model.

Examples

We conducted a synthetic PS shot gather experiment using a homogeneous model containing a single horizontal reflector at 4 km (vp = 3900 m/s, vs = 2300 m/s, eps = 0.2, del = 0.1, dip = 65, azimuth=30, Fpeak=7.5hz). Subsequently, we perturbed the background model to assess whether we could accurately recover the true model using FWI.

Figure 1 illustrates travel-time gradients based on a single shot gather as input data and a model featuring a single flat layer. Specifically, the gradient in panels 1a) and 1c) emphasizes high-frequency reflectivity contrasts. We referred to them as PS-FWI gradient as they were generated by conventional FWI imaging condition. In contrast, the gradient in panels 1b) and 1d) highlights low-frequency velocity differences, referred to as PS-RFWI gradient. Notably, the “rabbit ear” sensitivity kernel is visible in panel 1b), arising from the fact that this data originated from a single shot point. These individual kernels coherently sum across receivers in panel 1d), resulting in a smooth low-frequency update.

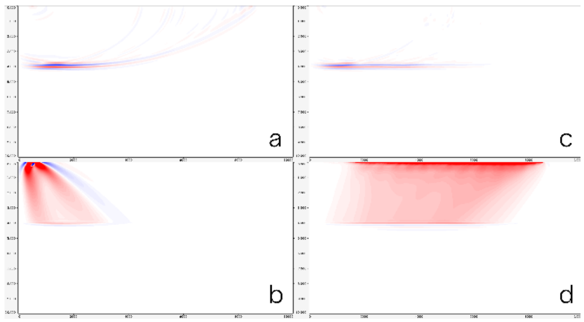

Figure 1: Single shot gradients of PS-FWI and PS-RFWI: a) PS-FWI gradient with S-leg on source-side; b) PS-RFWI gradient with S-leg on source-side; c) PS-FWI gradient with S-leg on receiver-side; and d) PS-RFWI gradient with S-leg on receiver-side.

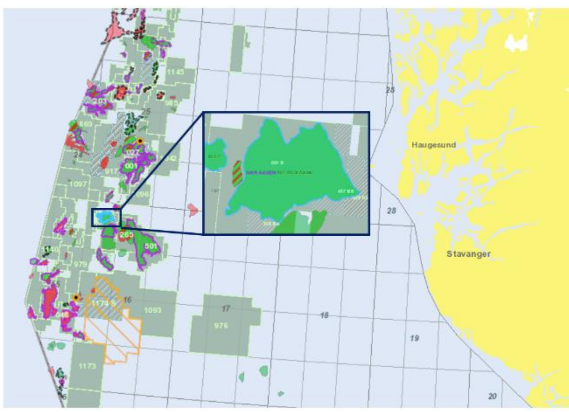

Figure 2: Ivar Aasen location in Norwegain North Sea (Source: modified from https://factmaps.sodir.no/factmaps/3_0.

We then applied the method to the Ivar Assen project acquired in North Sea. In 2019, Aker BP acquired the Ivar Aasen ocean-bottom cable dataset using inline-shooting geometry. The dataset consisted of 14 receiver lines (comprising 4096 receivers) in the northern part of the Ivar Aasen field (figure 2). The receiver line separation was 300 meters, with a receiver point interval of 25 meters. Both the shot line interval and shot point interval were 20 meters. The following signal processing steps were applied to the field's X and Y component datasets: deblending, noise Attenuation, rotation to radial component, radial down de-convolution and residual demultiple.

To initiate the PS-FWI process, an initial S-wave velocity (Vs) model is essential. Firstly, a high-resolution near-surface Vs model was derived by inverting dispersion curves obtained from Scholte waves. Next, we extracted a 1D Gamma function from well logs containing high-quality P- and S-sonic data. This function was then extended across the entire survey area, guided by horizon constraints. The Vp model was scaled using the Gamma field. Subsequently, it was merged with the surface wave-derived near-surface Vs model. This integration created the initial model, providing a comprehensive representation of subsurface properties. To refine the background Vs model, we employed three iterations of joint PP-PS tomography (Mathewson at al., 2015). These iterations focused on updating the Vs distribution, enhancing our understanding of the subsurface. We then applied our proposed method to update the Vs model with both low- and high-wavenumber components. We ran two bands of FWI with interleaved tomography, followed by pre-stack Kirchhoff depth migration (KDM) for intermediate quality control (see figure 3 for the processing flow). Figure 4 shows the PS-KDM images and Vs model at various stages. Specifically, 4c) and 4d) demonstrate that our proposed method effectively updates both the kinematics and high-resolution structures of the Vs model. This advancement promises improved accuracy and detailed subsurface information.

Conclusions

In this paper, we propose two approaches for full-waveform inversion using P-to-S converted waves to provide shear-velocity updates. Like PS-RTM, these approaches use the single-mode finite-shear acoustic TTI wave equations to solve for both P and S wave propagations with mode conversions controlled by a Born-approximation-based reflectivity model.

The first approach, referred to as PS-FWI, emphasizes sensitivity to the high-frequency component of the velocity model. It achieves this by utilizing the PS-RTM kernel to update the S-velocity model. This approach is particularly effective at resolving intricate details within the Vs model, which are crucial for FWI-derived reflectivity products. However, it does not address low-frequency kinematic updates.

In contrast, the second approach, referred to as PS-RFWI, incorporates a second Born modeling step for the S-propagation leg. This modification enhances sensitivity to the low-frequency components of the Vs model. Consequently, it provides the necessary kinematic updates for focusing PS images and aligning them with their PP counterparts. Field data examples demonstrate promising improvements in the shear velocity model, capturing both high-wavenumber details and low-wavenumber kinematics.

Acknowledgments

The authors thank the Ivar Aasen license operator Aker BP and the partners Equinor, Sval Energy, OKEA and M Vest Energy for their permission to publish the field data example. We also thank our colleagues at SLB including Wei Kang, Chirag Parekh, Olga Zdraveva, Sonika and Zhimei Yan for their support throughout this project. Additionally, particular thanks to Ole Edvard Aaker (Aker BP) for the valuable discussions.

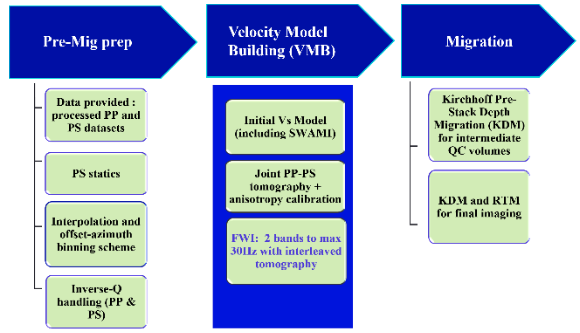

Figure 3: Processing flow. SWAMI is a surface wave-derived near-surface Vs model building approach.

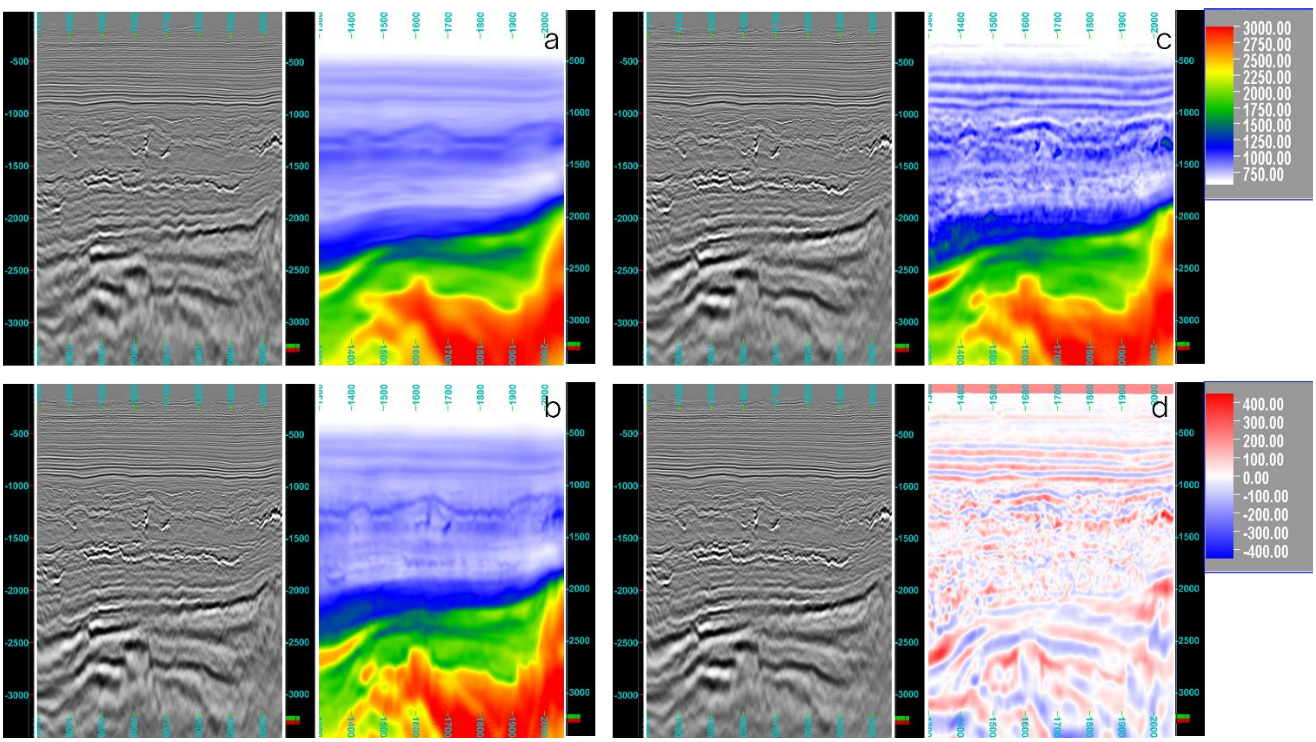

Figure 4: An inline result of Ivar Aasen. a) initial PS-KDM image and shear velocity; b) PS-KDM image and shear velocity after joint PP-PS tomography and anisotropy calibration; c) PS-KDM image and shear velocity after two bands of FWI and interleaved tomography; d) same PS-KDM image of c) and shear velocity update.